Effects of Graphite on the Corrosion Behavior of Aluminum-Graphite Composite in Sodium Chloride Solutions

El-Sayed M. Sherif [1,3,*], *A. A. Almajid* [1,2], *Fahamsyah Hamdan Latif* [1], *Harri Junaedi* [2]

[1] Center of Excellence for Research in Engineering Materials (CEREM), College of Engineering, King Saud University, P. O. Box 800, Al-Riyadh 11421, Saudi Arabia

[2] Department of Mechanical Engineering, College of Engineering, King Saud University, P.O. Box 800, Al-Riyadh 11421, Saudi Arabia

[3] Electrochemistry and Corrosion Laboratory, Department of Physical Chemistry, National Research Centre (NRC), Dokki, 12622 Cairo, Egypt
[*]E-mail: esherif@ksu.edu.sa

A series of different aluminum-graphite composites (Al-Gr), namely pure Al, Al-1%Gr, Al-2%Gr, and Al-3%Gr, was fabricated. The surface of these composites was investigated using optical microscopy to examine the distribution of exfoliated graphite within aluminum. The corrosion behavior of the pure Al and Al-Gr composites after different immersion intervals in 3.5% NaCl solutions was carried out using cyclic potentiodynamic polarization (CPP), chronoamperometry (CA), and electrochemical impedance spectroscopy (EIS). The study was also complimented by scanning electron microscopy (SEM) and energy dispersive X-ray (EDX) investigation. Corrosion measurements indicated that the presence of Gr and the increase of its content raise the corrosion rate and reduce the polarization resistance of Al. Increasing the immersion time of the test samples in the chloride solutions before measurements was found to decrease the general corrosion and increase the pitting corrosion. SEM/EDX investigations revealed that the presence of Gr activates the corrosion of Al due to the occurrence of galvanic corrosion and this effect increases with increasing Gr content.

1. INTRODUCTION

Aluminum and its alloys are widely used in a large number of industrial applications due to their excellent combination of properties, e.g. good corrosion resistance, excellent thermal conductivity, high strength to weight ratio, easy to deform, and high ductility. Aluminum alloys have

been generally used in manufacturing automobile and aircraft components because of high strength to weight ratio in order to make the moving vehicle lighter, which results in saving in fuel consumption, household appliances, containers, and electronic devices [1-3]. For these reasons, a number of investigations into its electrochemical behavior and corrosion resistance have been carried out in a wide variety of media [4-9].

In recent years the aerospace, military and automotive industries have been promoting the technological development of composite materials to achieve good mechanical strength/density and stiffness/density ratios [10, 11]. Composite materials usually refer to a combination of several materials that provide unique combination of properties which cannot be obtained by the individual constituents acting alone [12, 13]. The corrosion behaviour of the composites in the various environments that the material is likely to encounter is one important consideration when choosing a suitable material for a particular purpose. It has been established by various research studies that the corrosion behaviour of a metal-matrix composite is decided by numerous factors such as the composition of the alloy, the matrix microstructure, the dispersoid used, its size and distribution in the matrix, the nature of the interface between the dispersoid and the matrix, and even the technique adopted for preparing the composite [14-16]. Even a very small change in any one of these factors can seriously affect the corrosion characteristics of the material [13-18]. One of the main obstacles to the use of metal-matrix composites (MMCs) is the influence of reinforcement on corrosion resistance. This is particularly important in aluminium alloy based composites, where a protective oxide film imparts corrosion resistance. The addition of a reinforcing phase could lead to further discontinuities in the film, increasing the number of sites where corrosion can be initiated and rendering the composite liable to severe attack [19-22].

Graphite is well known as a solid lubricant and its presence in aluminium alloy matrices makes the alloy, self-lubricating. Aluminium alloys reinforced with graphite fibers are emerging as potential structural materials for aerospace needs and their outstanding mechanical properties have drawn considerable scientific attention to the exploration of their possible applicability to high-technology naval applications [23, 24]. Aluminium alloys dispersed with graphite particles are known as potential materials for tribiological applications such as bearings, bushings, pistons, etc [25-28]. The reason for the excellent tribiological properties of graphitic aluminium is that aluminium alloy matrix yields at low stresses and deforms extensively, which enhances the deformation and fragmentation of the surface and sub-surface graphite particles even after short running-in period. This provides a continuous film of graphite on the mating surfaces which, essentially, prevents metal to metal contact and hence prevents seizure.

The objective of this work was to study the effect of different percentages of graphite, namely 1, 2, and 3 %, on the corrosion behaviour of pure aluminium after their immersion for 40 min and 72 h in freely aerated 3.5% NaCl solutions. A particular attention was paid to the effect of graphite on the pitting corrosion of aluminum. To achieve this objective, the study was carried out using different electrochemical techniques such as cyclic potentiodynamic polarization, chronoamperometric current-time variations, and electrochemical impedance spectroscopy, along with optical microscopy, SEM, and EDX examinations.

2. EXPERIMENTAL PROCEDURE

2.1. Materials

The as received Al powder with purity of 99.9% and average particle size of 20 μm that used in this study was supplied by Riedel-De Haen Ag Seelze-Hannover, Germany. The exfoliated graphite with average diameter of 8 μm and thickness of 5-10 nm was supplied by Asbury Graphite Mills, USA.

2.2. Preparation of pure aluminium and Al-Gr composites

The concentration of exfoliated graphite in the composites was 0, 1, 2 and 3% by weight. First, the exfoliated graphite was dispersed in acetone using ultrasonic with the frequency of 50 kHz for 1 h. Then, the Al powder was slowly added into the solution and sonicated for 4 h to obtain a homogenous mixture. The mixtures were filtered and dried at 90°C for 6 h to form the powder. The powder was pressed at 520 MPa for 5 min to make a cylindrical shape with the ratio of 1:1 between diameter and height. The pressed samples were sintered at 500°C for 6 h in the furnace. The prepared composites were observed by a computer controlled optical microscopy (OM, Olympus, Model BX51M, Japanese made) to recognize the distribution of exfoliated graphite within aluminum.

2.3. Corrosion tests

2.3.1. Chemicals and electrochemical cell

A solution of 3.5% sodium chloride (NaCl, Merck, 99%), was prepared by dissolving 35 g of NaCl in 1 L glass flask. An electrochemical cell with a three-electrode configuration was used for electrochemical measurements. An Al electrode (either pure or containing different contents of Gr) was used as a working electrode.

A platinum foil and a Metrohm Ag/AgCl electrode (in 3 M KCl) were used as counter and reference electrodes, respectively.

The Al and Al-Gr rods for electrochemical measurements were prepared by welding a copper wire to a drilled hole was made on one face of the rod; the rod with the attached wire were then cold mounted in resin and left to dry in air for 24 h at room temperature.

Before measurements, the other face of the Al electrode, which was not drilled, was first grinded successively with metallographic emery paper of increasing fineness of up to 800 grits, and then polished with 1, 0.5 and 0.3μm alumina slurries (Buehler). The electrodes were then washed with doubly distilled water, degreased with acetone, washed using doubly distilled water again and finally dried with tissue paper. In order to prevent the possibility of crevice corrosion during measurement, the interface between sample and resin was coated with Bostik Quickset, a polyacrelate resin. The diameter of the working electrode was 1.2 cm with a total exposed surface area of 1.1304 cm^2.

2.3.2. Electrochemical methods

Electrochemical experiments were performed by using an Autolab Potentiostat (PGSTAT20 computer controlled) operated by the general purpose electrochemical software (GPES) version 4.9. The CPP curves were obtained by scanning the potential in the forward direction from -1800 to -500 mV against Ag/AgCl at a scan rate of 3.0mV/s; the potential was then reversed in the backward direction.

The values of the corrosion potential and corrosion current were obtained from the extrapolation of anodic and cathodic Tafel lines located next to the linearized current regions. The pitting potential was determined from the forward anodic polarization curves where a stable increase in the current density occurs. The protection potential was determined from the backward anodic polarization curve at the intersection point with the forward polarization curve. CA experiments were carried out by stepping the potential of the aluminum samples at − 600 mV versus Ag/AgCl for 2300 seconds. EIS tests were performed at corrosion potentials (E_{Corr}) over a frequency range of 100 kHz − 100 mHz, with an ac wave of ± 5 mV peak-to-peak overlaid on a dc bias potential, and the impedance data were collected using Powersine software at a rate of 10 points per decade change in frequency. All the electrochemical experiments were recorded after the electrode immersion in the test solution for 40 min and 72 h before measurements. All measurements were also carried out at room temperature in freely aerated solutions.

2.3.3. SEM investigation and EDX analysis

The SEM investigation and EDX analysis were obtained for the surface of Al and Al-Gr samples after their immersion in 3.5% NaCl solutions for 3 days. The SEM images were carried out by using a JEOL model JSM-6610LV (Japanese made) scanning electron microscope with an energy dispersive X-ray analyzer attached.

3. RESULTS AND DISCUSSION

3. 1. Optical microscopy (OM) investigation

Fig. 1 shows the optical micrograph of sintered Al and its composites. The sintered aluminum sample presents the grain size as shown in Fig. 1a. Al composite containing 1% of exfoliated graphite exhibits a homogenous microstructure; it was indicated from the distribution of exfoliated graphite within aluminum as shown Fig. 1b.

The exfoliated graphite was not uniformly distributed within aluminum because the agglomerates of exfoliated graphite can be found in the microstructure as shown in Fig. 1c and Fig. 1d. But the agglomerates in Fig. 1d is more obvious compared to Fig. 1c, this is due to high concentration of exfoliated graphite in Fig. 1d.
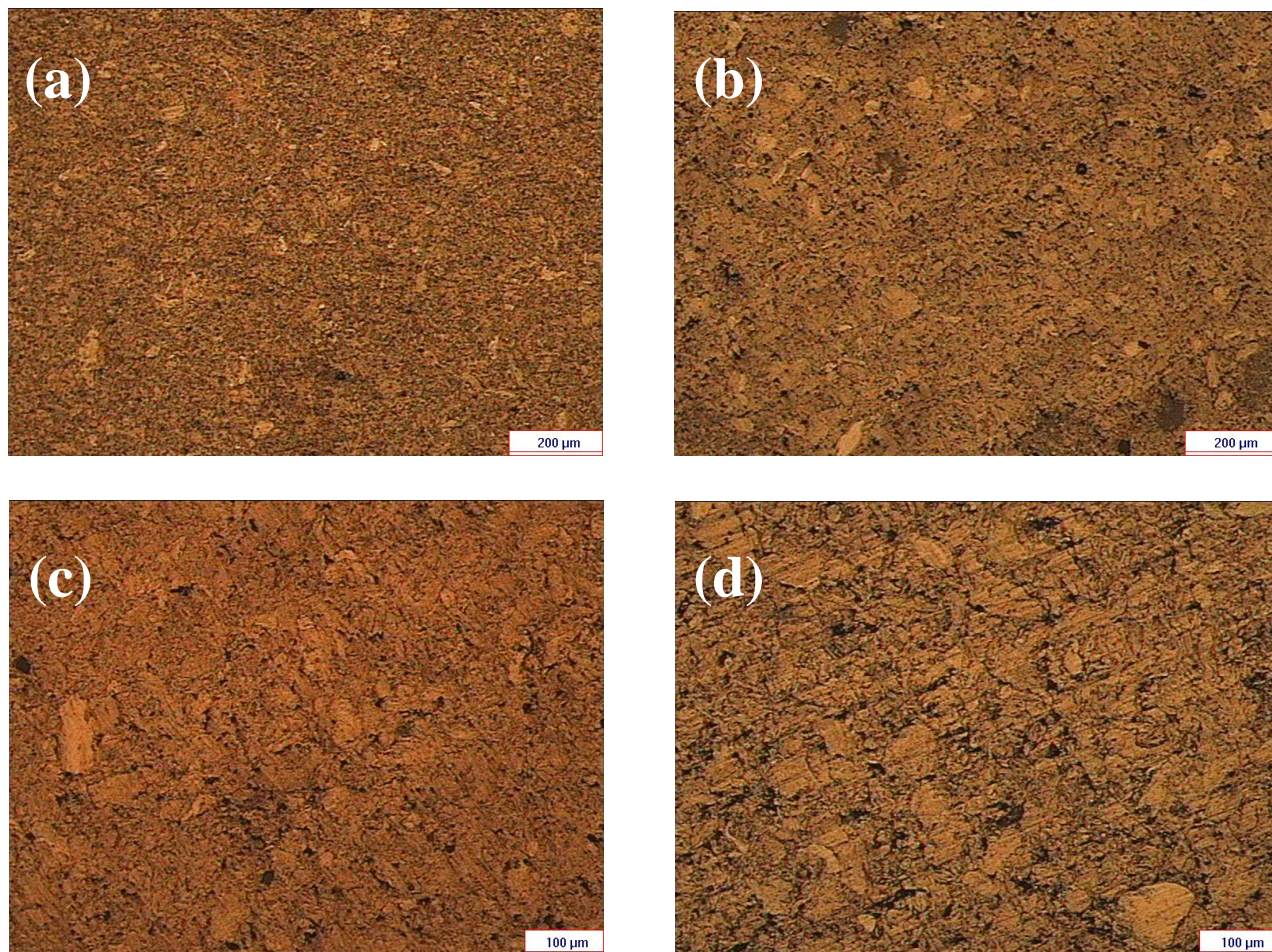
Figure 1. Optical micrographs of sintered Al and its composites (a) pure Al (b) Al-1%Gr (c) Al-2%Gr, and (d) Al-3%Gr.

3.2. Cyclic potentiodynamic polarization (CPP) data

In order to study the effect of Gr content on the corrosion behavior of pure Al, CPP experiments were carried out after 40 min and 72 h of the electrode immersion in the test solution before measurement. The CPP curves for (a) pure Al, (b) Al-1%Gr, (c) Al-2%Gr, and (d) Al-3%Gr after 40 min and 72 h immersion in 3.5% NaCl solutions are shown in Fig. 2 and Fig. 3, respectively. It is generally agreed that the cathodic reaction for Al in aerated near neutral pH solutions is the oxygen reduction followed by its adsorption [7, 8], i.e.

$$\frac{1}{2}O_2 + H_2O_{(S)} + e^- = OH_{ads.} + OH^- \tag{1}$$
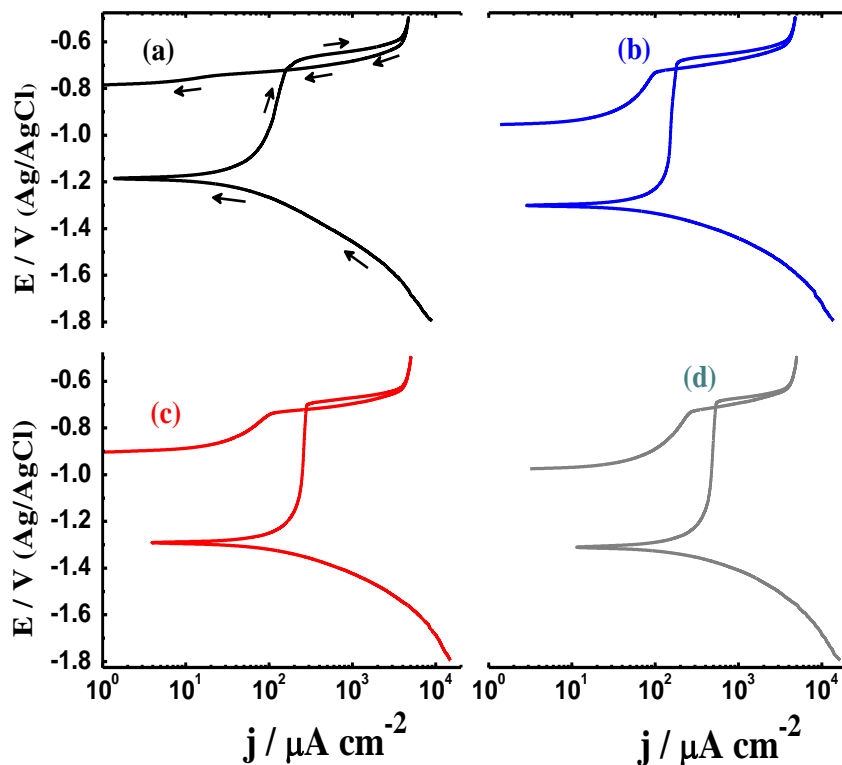
and

$$OH_{ads.} + e^- = OH^- \tag{2}$$
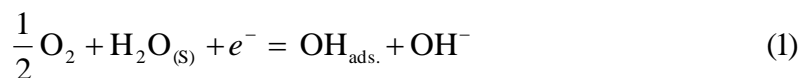
Figure 2. Cyclic potentiodynamic polarization for (a) pure Al, (b) Al-1%Gr, (c) Al-2%Gr, and (d) Al-3%Gr after 40 min immersion in 3.5% NaCl solutions.
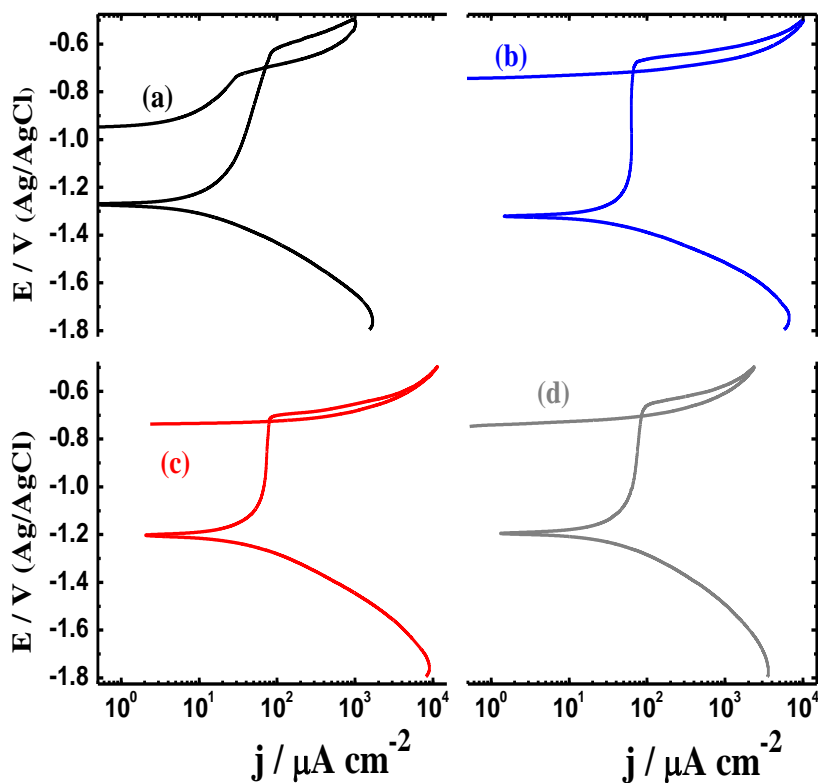

Figure 3. Cyclic potentiodynamic polarization for (a) pure Al, (b) Al-1%Gr, (c) Al-2%Gr, and (d) Al-3%Gr after 72 h immersion in 3.5% NaCl solutions.

On the other hand, the anodic reaction of Al (Fig. 2 and Fig. 3, curves a) started from the corrosion potential that was recorded at a more negative value, -1180 mV, followed by a passive region at an average current density of 124 $\mu A/cm^2$, extending from -1100 to -710 mV (after 40 min, Fig. 2, curve a) and -1285 mV, 44.5 $\mu A/cm^2$, extending from -1200 to -650 mV (after 72 h, Fig. 2, curve a). In this potential range, aluminum oxide is formed on the surface according to the reaction,

$$Al_{(S)} + 3OH^- = Al(OH)_{3,ads.} + 3e^- \tag{3}$$
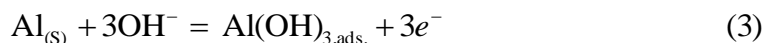
The aluminum hydroxide, $Al(OH)_3$, is transformed to $Al_2O_3.3H_2O$,

$$Al(OH)_{3,ads.} = Al_2O_3.3H_2O \tag{4}$$

It is worth mentioning that Al_2O_3 is of a dual nature and consists of an adherent, compact, and stable inner oxide film covered with a porous, less stable outer layer, which is more susceptible to corrosion [29, 30, 31]. This explains the observed abrupt increase in the current values after increasing the applied potential, which leads with the aid of the chloride ions attack on the flawed areas of the oxide film to the breakdown of the passive layer and occurrence of pitting corrosion as follows [7, 8, 32, 33],

$$Al = Al^{3+}. + 3e^- \tag{5}$$

and

$$Al^{3+} + 4Cl^- = AlCl_4^- \tag{6}$$

It has been reported [33, 34] that a salt barrier of $AlCl_3$ is formed within the pits on their formation, which could then form $AlCl_4^-$ (Reaction 6), and diffuses into the bulk of the solution. On the other hand, it has been proposed [35] that the chloride ions do not enter into the oxide film but they are chemisorbed onto the oxide surface and act as a reaction partner, aiding the oxide to dissolve via the formation of oxychloride complexes.

$$Al^{3+}{}_{(in\ crystal\ lattice\ of\ the\ oxide)} + 2Cl^- + 2OH^- = Al(OH)_2Cl_2^- \tag{7}$$
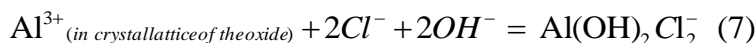
The values of the corrosion potential (E_{Corr}), corrosion current (j_{Corr}), cathodic Tafel slope (βc), anodic Tafel slope (βa), passivation current (j_{Pass}), pitting potential (E_{Pit}), pitting current (j_{Pit}), polarization resistance (R_P), and corrosion rate (K_{Corr}) for pure Al and Al-Gr composites after their immersion in 3.5% NaCl solutions for 40 min and 72 h obtained from CPP curves (Fig. 2 and Fig. 3) are shown in Table 1.

Table 1. Corrosion parameters obtained from polarization curves shown in Fig. 2 and Fig. 3 for the different Al electrodes after 40 min and 72 h of its immersion in 3.5% NaCl solutions.

Aluminum	Parameter								
	β_c/ mV dec^{-1}	E_{Corr}/ mV	j_{Corr}/ μA cm^{-2}	β_a/ mV dec^{-1}	j_{Pass}/ μA cm^{-2}	E_{Prot}/ mV	E_{Pit}/ mV	R_p/ Ω cm^2	K_{Corr}/ mmy^{-1}
Al-0Gr (40 min)	−150	−1175	32	180	124	−710	−670	1.11	0.35
Al-1Gr (40 min)	−145	−1260	70	170	155	−715	−675	0.49	0.76
Al-2Gr (40 min)	−140	−1270	95	165	255	−715	−685	0.35	1.04
Al-3Gr (40 min)	−130	−1300	170	160	481	−712	−690	0.18	1.85
Al-0Gr (72 h)	−160	−1285	8.5	220	44.6	−700	−650	4.74	0.09
Al-1Gr (72 h)	−155	−1275	23	200	62.9	−720	−670	1.65	0.25
Al-2Gr (72 h)	−155	−1185	25	180	72.6	−725	−700	1.45	0.27
Al-3Gr (72 h)	−150	−1180	27	170	73.6	−705	−680	1.28	0.29

The values of R_P and K_{Corr} were calculated from the polarization data as reported in our previous work [36-45]. It is subtly seen from Fig. 2, Fig. 3 and Table 1 that the presence of Gr and the increase of its content within Al shifted βc and E_{Corr} to more negative values, increased the values of j_{Corr}, $j_{Pass,}$ and K_{Corr}, and decreased the values of R_P, which indicates on the activation of Al by Gr and this effect increases with increasing the Gr content. According to Saxena et al. [46], the higher corrosion rate of Al-Gr composite than the aluminum itself is possibly due to the graphite particles being cathodic relative to the matrix thus leading to galvanic corrosion in the presence of an electrolyte. Increasing the immersion time to 72 h as shown in Fig. 3, shifts E_{Corr} towards the negative direction and decreases the uniform corrosion of both pure Al and Al-Gr composites. This can be seen from the low values of j_{Corr}, $j_{Pass,}$ and K_{Corr}, and the high values of Rp, which is probably due to either increasing the thickness of the passive oxide film, Al_2O_3 or the accumulation of corrosion products on the electrode surface.

3.3. Chronoamperometric (CA) measurements and SEM/EDX investigations

In order to shed more light on the pitting corrosion of Al and Al-Gr composites in 3.5% NaCl solutions at a less negative potential value, chronoamperometric experiments were carried out. Fig. 4. exhibits the variation of the measured dissolution currents versus time for Al and Al-Gr composites that were immersed in the 3.5% NaCl solutions for (a) 40 min and (b) 72 h, respectively before stepping the potential to - 600 mV vs. Ag/AgCl. It is seen from Fig. 4a that the lowest current values were recorded for the pure Al, where the current increased upon applying the potential in the first few seconds, the current then decreased slowly with time for the whole time of the experiment. For Al-Gr composites, the current-time recorded the same behavior with increased absolute current with increasing the Gr content in the composites. The CA curves at this condition do not indicate on the

occurrence of pitting corrosion but prove that the presence of Gr and the increase of its content enhance the anodic dissolution of Al in the chloride solution.
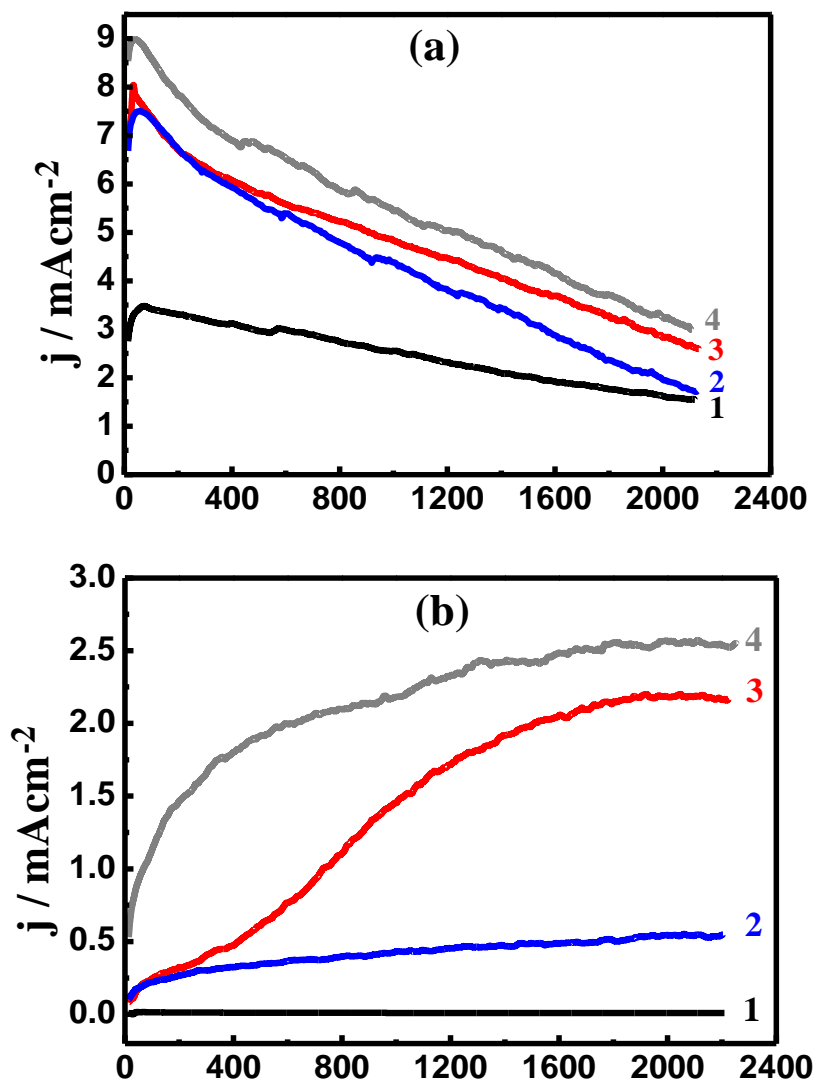

Figure 4. Chronoamperometric current-time curves obtained for (1) Al, (2) Al-1%Gr, (3) Al-2%Gr, and (4) Al-3%Gr, at − 600 mV vs. Ag/AgCl after (a) 40 min and (b) 72 h immersion in 3.5% NaCl solutions.

Increasing the immersion time to 72 h, Fig. 4b, showed that the current recorded very low values with time for the pure aluminum, curve 1. This is because the long immersion time allows Al to develop thick and compact oxide film and/or a layer of corrosion products that cover up the Al surface and protect it from dissolution. On the other hand, the increase of current values with time for Al-Gr composites is due to the dissolution of the film formed on their surfaces, while they were immersed in the chloride solution, leading to the occurrence of the pitting corrosion. It is seen from Fig. 4b (curves 2-4) also that the increase of Gr content in the composite increases the absolute current of the electrode

with time, which in turn increases the severity of pitting corrosion. This was confirmed by the SEM/EDX investigations for Al and Al-Gr composites at the same condition.
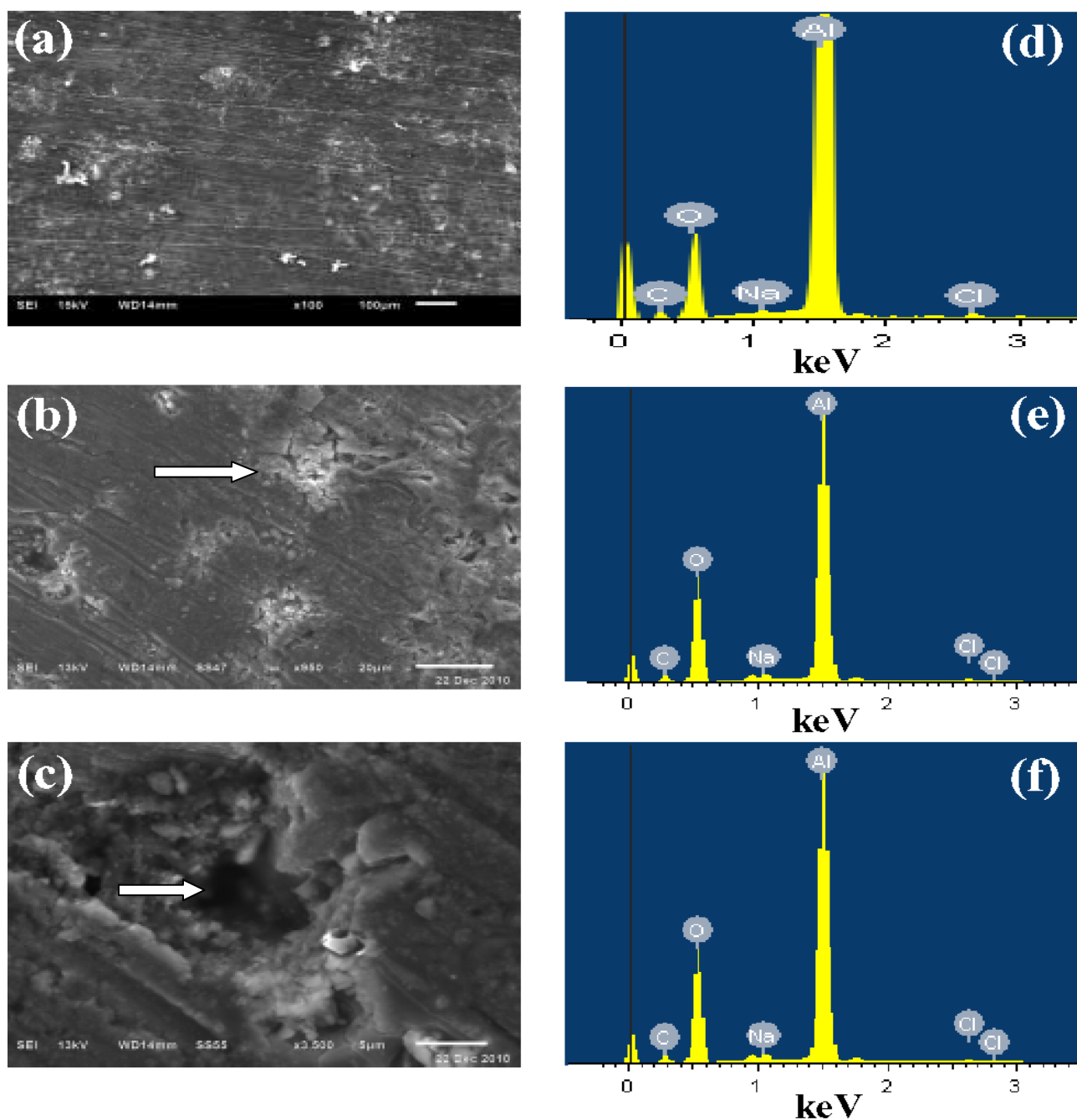

Figure 5. SEM micrographs for (a) pure Al, (b) Al-3%Gr, (c) an expanded area of image b shows the shape of a pit, after 72 h immersion in 3.5% NaCl solutions before applying – 600 mV vs. Ag/AgCl for 2300 sec; (d), (e) and (f) represent the corresponding EDX profile analysis for the surfaces shown in the micrographs (a), (b), and (c), respectively.

Fig. 5 shows the obtained SEM micrographs for (a) pure Al, (b) Al-3%Gr, (c) an expanded area of image (b) shows the shape of a pit, after 72 h immersion in 3.5% NaCl solutions before applying –

600 mV vs. Ag/AgCl for 2300 sec; (d), (e) and (f) represent the corresponding EDX profile analysis for the surfaces shown in the micrographs (a), (b), and (c), respectively. It is not clear from the SEM image (a) that the surface does have pits but corrosion products.
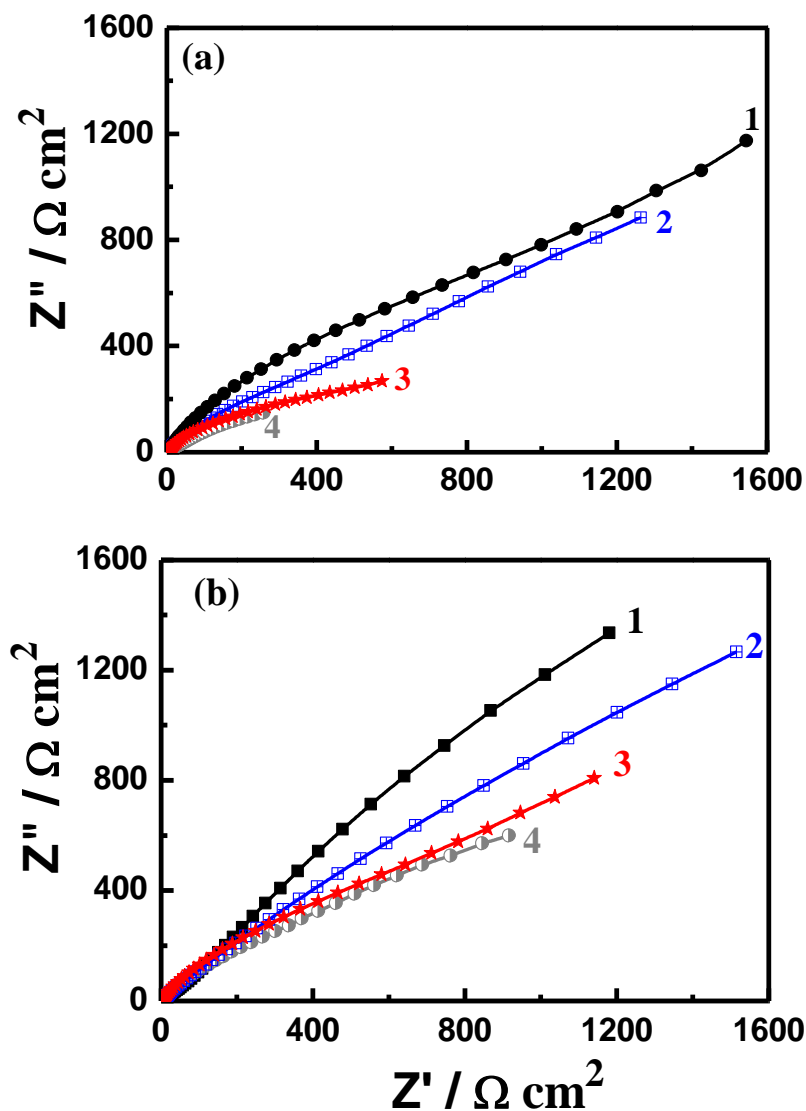

Figure 6. EIS Nyquist plots for (a) pure Al, (b) Al-1%Gr, (c) Al-2%Gr, and (d) Al-3%Gr, after their immersion in 3.5% NaCl solutions for (a) 40 min and (b) 72 h.

The corresponding EDX profile analysis shown in Fig. 5d provided that the atomic percentages of the elements found on the Al surface were 65.16% Al, 32.10% O, 2.21% C, 0.32% Cl, and 0.21% Na. This indicates that the compound that may be found on the surface is mainly aluminum oxide with traces of sodium chloride salt. While for Al-3%Gr, SEM image, Fig. 5b, shows several pits; some of them are covered with corrosion products. The EDX analysis for the corrosion products formed on the pits is shown in Fig. 5e from which the atomic percentage of oxygen was the highest. Where, 52.64% O, 32.20% Al, 14.22% C, 0.59% Na, and 0.35% Cl were found in the layer. The high content of O is

due to the formation of Al_2O_3 on the top of the pits as the main compound on the surface. The presence of low Al percentage is as a result of its dissolution under the high applied potential, -600 mV vs. Ag/AgCl. The presence of carbon might have come from the Al-Gr composite itself. The low content of Na and Cl indicates that the presence of NaCl salt was deposited on the composite surface during its immersion in the test solution. In order to give a close looking at the pit shape and compounds that might form inside it, the SEM and EDX investigations for Al-3%Gr composite were carried out as shown in Fig. 5c and Fig. 5f, respectively. The atomic percentages of the elements recorded in the EDX profile were 59.74% C, 21.32% Al, 18.54% O, and 0.40% Cl without Na. The low content of Al and the high percentage of C inside the pit prove that a selective dissolution of Al occurs due to the galvanic corrosion [46]. It has been reported that [47, 48] pits develop at sites where oxygen adsorbed on the composite surface is displaced by an aggressive species such as Cl^- ions that are presented in the test solution. This is because Cl^- ions have small diameters allow it to penetrate through the protective oxide film and displace oxygen at the sites where metal-oxygen bond is the weakest.

3.5. Electrochemical impedance spectroscopy (EIS) measurements

The EIS measurements were carried out to determine kinetic parameters for electron transfer reactions at the Al and Al-Gr composites/electrolyte interface and to confirm the data obtained by polarization and chronoamperometric measurements.

Table 2. EIS parameters obtained by fitting the Nyquist plots shown in Fig. 6 with the equivalent circuit shown in Fig. 7 for the Al and Al-Gr composites in aerated 3.5% NaCl solutions.

Parameter Alloy	R_S / Ωcm^2	C_{dl} / μF cm^{-2}	R_{p1} / Ω cm^2	Q		R_{p2} / Ω cm^2	W / $\Omega^{-1}cm^{-2}$
				Y_Q / $\mu F\, cm^{-2}$	n		
Al-0Gr (40 min)	6.352	6.67	124.2	11.77	0.80	1241	71 x 10^{-6}
Al-1Gr (40 min)	5.823	15.5	85.61	18.32	0.80	1027	81 x 10^{-6}
Al-2Gr (40 min)	5.634	20.2	60.38	34.05	0.60	798.9	89 x 10^{-6}
Al-3Gr (40 min)	5.304	24.0	45.67	56.34	0.44	655.3	93 x 10^{-6}
Al-0Gr (72 h)	8.813	3.02	148.3	8.334	0.64	1408	35 x 10^{-6}
Al-1Gr (72 h)	7.518	4.99	89.65	14.22	0.58	1294	41 x 10^{-6}
Al-2Gr (72 h)	6.487	11.04	68.83	33.17	0.65	907.8	65 x 10^{-6}
Al-3Gr (72 h)	5.691	15.54	58.69	45.81	0.62	756.4	76 x 10^{-6}

The method has successfully employed to explain the corrosion and corrosion inhibition of several metals and alloys in chloride media [7, 8, 36-41, 43-45, 49-51]. In order to determine the

impedance characteristics at the electrode/electrolyte interface under various experimental conditions, we carried out EIS measurements. The EIS Nyquist plots for (1) pure Al, (2) Al-1%Gr, (3) Al-2%Gr, and (4) Al-3%Gr, after their immersion in 3.5% NaCl solutions for (a) 40 min and (b) 72 h, respectively are shown in Fig. 6. The EIS data shown in Fig. 6 were analysed by fitting to the equivalent circuit model shown in Fig. 7. The parameters obtained by fitting the equivalent circuit are listed in Table 2. Here, R_S represents the solution resistance between the working (Al and Al-Gr composites) electrode and the counter (platinum) electrode, C_{dl} the double layer capacitance, R_{p1} the polarization resistance for the charge transfer through the film (aluminum oxide and/or corrosion products), Q the constant phase elements (*CPEs*) and contain two parameters; a pseudo capacitance and an exponent (an exponent of less than unity indicates a dispersion of capacitor effects [52]), R_{p2} another polarization resistance at the film/electrolyte interface and can be defined also as the charge transfer resistance, and W the Warburg impedance.
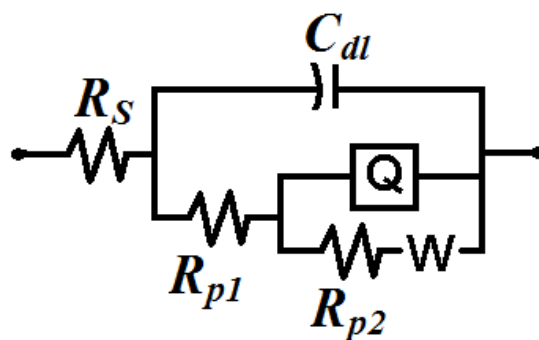

Figure 7. The equivalent circuit used to fit the experimental data presented in Fig. 6. See text for symbols used in the circuit.

It is seen from Fig. 6a and Table 2 that the solution and polarization resistances, Rs as well as both R_{p1} and R_{p2}, decrease as Gr content is increased. The same effect was noticed when the immersion time was increased to 72 h with higher values of surface and polarization resistances, in good agreement with those obtained by potentiodynamic polarization (Fig. 2, Fig. 3 and Table 1), and current–time (Fig. 4) methods. Where, their increase with increasing time is attributed to the formation of a passive film and/or corrosion product, which gets thicker with time and could lead to the decrease in j_{Corr} and K_{Corr} and also the increase in R_P values we have seen in polarization data under the same conditions. The semicircles at high frequencies in Fig. 6 are generally associated with the relaxation of electrical double layer capacitors and the diameters of the high frequency semicircles can be considered as the charge transfer resistance ($R_P = R_{P2} + R_{P2}$) [38]. The increase in the double layer capacitance (Cdl) upon increase in Gr content due to the enhanced access of charged species to the surface suggest that the mass transport increases and so dissolution of Al increases. The constant phase elements (CPEs, Q) with their n values close to 1.0 represent double layer capacitors with some pores; the CPEs increase and their n values decrease in the presence of Gr and upon increase in its concentration, which indicates the increased dissolution of Al. The presence of the Warburg (*W)*

impedance might indicate that the mass transport is limited by the surface oxide layer but this effect decreases in the presence of Gr and the increase of its content as shown in Table 2.

4. CONCLUSIONS

The effect of adding 1%Gr, 2%Gr, and 3%Gr on the corrosion behavior of pure Al in 3.5% NaCl solution was investigated by electrochemical and spectroscopic techniques. CPP measurements showed that the presence of Gr and the increase of its content with Al increased the corrosion current, corrosion rate and decreased the polarization resistance. Chronoamperometric current-time experiments at − 600 mV vs. Ag/AgCl for 2300 sec revealed that the dissolution current of Al increased with Gr content. Impedance spectra confirmed the data obtained by polarization and the change of current with time at constant potential and indicated that the values of solution and polarization resistances decreased in the presence of Gr and the increase of its percentage. All electrochemical investigations indicated that the dissolution of Al for all electrodes (in absence and presence of Gr) decreased when the immersion time before measurements was increased from 40 min to 72 h. SEM images taken on the surface of pure Al and Al-3%Gr proved that pitting corrosion is more severe for Al-Gr composite. EDX profile analysis revealed that the reason for the high corrosion of Al-Gr composites compared to pure Al is due to the selective dissolution of Al. The dissolution of Al is influenced by the force of galvanic corrosion, where Gr acts as the cathode due to its more noble potential than Al, which has very active potential.

References

1. G. A. Capauano, W. G. Davenport, *J. Electrochem. Soc.*, 118 (1971) 1688.
2. P. Fellener, M. C. Paucivova, K. Mataisovsky, *Surf. Coat. Technol.*, 14 (1981) 101.
3. F.S. Mohammad, E.A.H. Al Zubaidy, G. Bassioni, *Int. J. Electrochem. Sci.*, 6 (2011) 222.
4. Fang Wang, Yabin Wang, Yanni Li, *Int. J. Electrochem. Sci.,* 6 (2011) 793.
5. W.R. Osório, N. Cheung, L.C. Peixoto, A. Garcia, *Int. J. Electrochem. Sci.,* 4 (2009) 820.
6. J. W. Diggle, T. C. Downie, C. Goulding, *Electrochim. Acta,* 15 (1970) 1079.
7. E. M. Sherif, S.-M. Park, *Electrochim. Acta*, 51 (2006) 1313.
8. E. M. Sherif, S.-M. Park, *J. Electrochem. Soc.,* 152 (2005) B205.
9. I.B. Obot, N.O. Obi-Egbedi, S.A. Umoren, E.E. Ebenso, *Int. J. Electrochem. Sci.,* 5 (2010) 994.
10. A.Pardo, M. C. Merino, S. Merino, M. D. Lo´pez, F. Viejo, M. Carboneras, *Mater. Corros.*, 54 (2003) 311.
11. P. Rohatgi, *JOM (J. Miner. Met. Mater. Soc.)*, 43 (4) (1991) 10.
12. A.Pardo, M. C. Merino, S. Merino, F. Viejo, M. Carbonera, R. Arrabal, *Corros. Sci.*, 47 (2005) 1750–1764.
13. A.P. Divecha, S. G. Fishman, S. D. Karmakar, *J. Metals,* 33 (1981) 12.

14. K. H. W. Seah, S.C. Sharma, B. M. Girish, *Corros. Sci.*, 39 (1997) 1-7.
15. G. M. Pinto, J. Nayak, A. N. Shetty, *Int. J. Electrochem. Sci.,* 4 (2009) 1452.
16. S. L. Pohlman, *Corrosion*, 34 (1978).
17. P. R. Gibson, A. J. Clegg, A. A. Das, *Mater. Technol.*, 1 (1985) 559.
18. D. M. Aylor, P. J. Moran, *J. Electrochem. Soc.,* 132 (1985) 1277.
19. S. L. Pohlman, *Corrosion*, 34 (1978) 156.
20. A.J. Trowsdale, B. Noble, S. J. Harris, I. S. R. Gibbins, G. E. Thompson, G. C. Wood, *Corros. Sci.,* 38 (1996) 177.
21. R. C. Paciej, V. S. Agarwala, *Corrosion*, 42 (1986) 718.
22. P. P. Trzaskoma, E. McCafferty, C. R. Crowe, *J. Electrochem. Soc.*, 130 (1983) 1804.
23. A.J. Griffiths, A. Turnbull, *Corros. Sci.*, 36 (1994) 23.
24. D. M. Aylor, R. J. Ferrara, R. M. Kain, *Mater. Perform.*, 23 (1984) 32.
25. M. G. Vassilaros, D. A. Davis, G. L. Stecker, J. P. Gudas, in *"Proceedings of the Tri-Service Conference on Corrosion",* US Air Force, Academy, Colorado, November 1980, Vol. II.
26. A.I. Onen, B.T. Nwufo, E.E. Ebenso, R.M. Hlophe, *Int. J. Electrochem. Sci.,* 5 (2010) 1563.
27. N. A. P. Rao, S. Biswas, P. K. Rohatgi, A. Santhanam, K. Narayanaswamy, *Tribo. Int.*, 13 (1980) 171.
28. M. Saxena, B. K. Prasad, T. K. Dan, *J. Mater. Sci.*, 27 (1992) 4805-4812.
29. G. Y. Elewady, I .A. El-Said, A.S.Fouda, *Int. J. Electrochem. Sci.,* 3 (2008) 177.
30. F. D. Wall, M. A. Martinez, J. J. Vandenavyle, *J. Electrochem. Soc.,* 151 (2004) B354.
31. C. M. A. Brett, I. A. R. Gomes, J. P. S. Martins, *Corros. Sci.,* 36 (1994) 915.
32. W. Diggle, T. C. Downie, C. Goulding, *Electrochim. Acta,* 15 (1970) 1079.
33. N. Sato, *Corros. Sci.*, 37 (1995) 1947.
34. F. Hunkeler, G. S. Frankel, H. Bohni, *Corrosion (Houston),* 43 (1987) 189.
35. L. Tomcsanyi, K. Varga, I. Bartik, G. Horanyi, E. Maleczki, *Electrochim. Acta,* 34 (1989) 855.
36. E. M. Sherif, S.-M. Park, *Corros. Sci.*, 48 (2006) 4065.
37. E. M. Sherif, S.-M. Park, *J. Electrochem. Soc.*, 152 (2005) B428.
38. E. M. Sherif, S.-M. Park, *Electrochim. Acta,* 51 (2006) 6556.
39. E. M. Sherif, J. H. Potgieter, J. D. Comins, L. Cornish, P. A. Olubambi, C. N. Machio, *J. Appl. Electrochem.,* 39 (2009) 1385.
40. E. M. Sherif, J. H. Potgieter, J. D. Comins, L. Cornish, P. A. Olubambi, C. N. Machio, *Corros. Sci.,* 51 (2009) 1364.
41. E. M. Sherif, A. A Almajid, *J. Appl. Electrochem.*, 40 (2010) 1555.
42. E. M. Sherif, R. M. Erasmus, J. D. Comins, *J. Electrochim. Acta,* 55 (2010) 3657.
43. E. M. Sherif, R. M. Erasmus, J. D. Comins, *J. Appl. Electrochem.*, 39 (2009) 83.
44. E. M. Sherif, R. M. Erasmus, J. D. Comins, *Corros. Sci.*, 50 (2008) 3439.
45. E. M. Sherif, R. M. Erasmus, J. D. Comins, *J. Colloid Inter. Sci.*, 209 (2007) 470.
46. M. Saxena, O. P. Modi, A. H. Yegneswaran, P. K. Rohatgi, *Corros. Sci.*, 27 (1987) 249-252, 254-256.
47. H. Bohni, H. H. Uhlig, *J. Electrochem. Soc.*, 116 (1969) 906.
48. V. K. Gouda, I. Z. Selim, A. A. Khedr, A. M. Fathi, *J. Mater. Sci. Technol.*, 15 (1999) 208.
49. E. M. Sherif, S.-M. Park, *J. Electrochim. Acta,* 51 (2006) 4665.
50. E. M. Sherif, R. M. Erasmus, J. D. Comins, *J. Colloid Interface Sci.*, 306 (2007) 96.
51. E. M. Sherif, R. M. Erasmus, J. D. Comins, *J. Colloid Interface Sci.,* 311 (2007) 144.
52. R. D. Klassen and P. R. Roberge, Y. Wang, *Corrosion, Paper No. 05232*, NACE International, Houston, Texas (2005).